Article ID: 1006-8775(2012) 02-0195-12

BOUNDARY LAYER STRUCTURE IN TYPHOON SAOMAI (2006): UNDERSTANDING THE EFFECTS OF EXCHANGE COEFFICIENT

MING Jie (明　杰)[1], SONG Jin-jie (宋金杰)[1], CHEN Bao-jun (陈宝君)[1], WANG Ke-fa (王可发)[2]

(1. Key Laboratory of Mesoscale Severe Weather and School of Atmospheric Sciences, Nanjing University, Nanjing 210093 China; 2. Climate Center, Meteorological Bureau of Jiangsu Province, Nanjing 210008 China)

Abstract: Recent studies have shown that surface fluxes and exchange coefficients are particularly important to models attempting to simulate the evolution and maintenance of hurricanes or typhoons. By using an advanced research version of the Weather Research and Forecasting (ARW) modeling system, this work aims to study the impact of modified exchange coefficient on the intensity and structures of typhoon Saomai (2006) over the western North Pacific. Numerical experiments with the modified and unmodified exchange coefficients are used to investigate the intensity and structure of the storm, especially the structures of the boundary layer within the storm. Results show that, compared to the unmodified experiment, the simulated typhoon in the modified experiment has a bigger deepening rate after 30-h and is the same as the observation in the last 12-h. The roughness is leveled off when wind speed is greater than 30 m/s. The momentum exchange coefficient (C_D) and enthalpy exchange coefficient (C_K) are leveled off too, and C_D is decreased more than C_K when wind speed is greater than 30 m/s. More sensible heat flux and less latent heat flux are produced. In the lower level, the modified experiment has slightly stronger outflow, stronger vertical gradient of equivalent potential temperature and substantially higher maximum tangential winds than the unmodified experiment has. The modified experiment generates larger wind speed and water vapor tendencies and transports more air of high equivalent potential temperature to the eyewall in the boundary layer. It induces more and strong convection in the eyewall, thereby leading to a stronger storm.

Key words: typhoon; Saomai; roughness; exchange coefficient; boundary layer

CLC number: P444 **Document code:** A **doi:** 10.3969/j.issn.1006-8775.2012.02.009

1 INTRODUCTION

It has long been recognized that the boundary layer plays an important role in the development of tropical storms. Tropical cyclones interact with the ocean through the boundary layer, obtaining heat and moisture, and transferring momentum to the ocean in the form of currents and waves. On one hand, surface fluxes of sensible and latent heat are very important in the development and maintenance of tropical cyclones. Malkus and Riehl[1] showed that surface fluxes in the inner core of hurricanes are capable of increasing the equivalent potential temperature by more than 10 K, which contributes significantly to deepen the pressure of hurricanes. Ooyama[2] suggested that surface fluxes in the outer region of hurricanes are also necessary for maintaining the equivalent potential temperature against the effects of entrainment of subsiding dry air into the planetary boundary layer. Emanuel[3] and Rotunno and Emanuel[4] further demonstrated the importance of surface fluxes by showing that hurricanes can develop and maintain with the energy derived from surface fluxes of sensible and latent heat in environments free of convective available potential energy (CAPE). On the other hand, the dependence of the potential intensity on the surface heat and momentum exchange coefficients was suggested to be important too. Ooyama[2], Rosenthal[5], and Emanuel[3], using numerical and mathematical models, confirmed that the potential intensity of hurricanes increases with increases in the heat exchange coefficient (C_H) and decreases with decreases in the momentum exchange coefficient (C_D). In other words, hurricanes become stronger as the transfer of sensible and latent

Received 2011-09-30; **Revised** 2012-02-16; **Accepted** 2012-04-15

Foundation item: National Natural Science Foundation of China (40730948, 40830958, 41105035, 40921160382); National Grand Fundamental Research 973 Program of China (2009CB421502); social commonweal research program (GYHY201006007)

Biography: MING Jie, Lecturer, primarily undertaking research on mesoscale meteorology and numerical experiment.

Corresponding author: CHEN Bao-jun, e-mail: bjchen@nju.edu.cn

heat from the sea surface is increased and becomes weaker as the frictional dissipation is increased. It also has been demonstrated that hurricane intensity in both idealized, axisymmetric, quasi-balanced models (Emanuel[6]) and "full-physics" nonhydrostatic models (Braun and Tao[7]) exhibits significant sensitivity to the ratio of the bulk exchange coefficient for enthalpy flux (C_K) to the exchange coefficient for momentum. Based on the comparison of model predictions with observations of the hurricane intensity for a number of hurricanes, Emanuel[6] concluded that the ratio of C_K/C_D lies in the range 1.2–1.5 in the high wind regime and suggests 0.75 as a lowest threshold to ensure model consistence and the intensity of a hurricane increases as the ratio of the exchange coefficients for enthalpy and momentum (C_K/C_D) increases. Furthermore, the laboratory work by Donelan et al.[8] found C_D to reach a maximum at wind speeds around 35 m/s before leveling off. The authors attribute this to increased sheltering of the wind behind steeper waves. These results support those of Powell et al.[9] based on extrapolating GPS dropsonde profiles to the surface.

Surface fluxes and exchange coefficients are particularly important to models attempting to simulate the evolution and maintenance of hurricanes or typhoons. It is important to understand how they regarding the characters within the boundary layer impact experiments of hurricanes or typhoons. Unfortunately, few works have been undertaken to study the relationship between the exchange coefficients and the intensity of typhoon in western North Pacific. The purpose of this work is to study the impact of modified exchange coefficient on the intensity and structures of Typhoon Saomai (2006) over the western North Pacific. In addition, the sensitivity of experiments to different formulations of the exchange coefficient is investigated too. The paper is organized as follows. Section 2 and 3 includes a brief overview of Typhoon Saomai, a description of the numerical model and experimental design. Numerical results are verified to various observations in section 4. And the simulated typhoon intensity and structures are examined in section 5. Concluding remarks and discussion are drawn in section 6.

2 A BRIEF OVERVIEW OF TYPHOON SAOMAI (2006)

Typhoon Saomai (2006) originated from a tropical disturbance near the east of Chuuk on 31 July. It gradually increased in organization over the next several days as it moved northwestward. The system formed a tropical depression near the southeast of Guam on 4 August 2006. Saomai was facing toward the East China Sea and moving northwestward. It intensified quickly and reached typhoon intensity by 0600 UTC 7 August, with a central location at 18.8°N, 138.2°E. The typhoon continued to intensify rapidly, and became a super typhoon with a maximum wind speed of 51.4 m/s at 0600 UTC 9 August. Subsequently, Saomai made a landfall on Cangnan of Zhejiang province at 1100 UTC 10 August and then moved westward and passed through Fujian province. It reduced to a tropical storm within Geyang of Jiangxi province one day later. Finally, it weakened to a depression in Hubei province.

When Saomai made landfall on Zhejiang province, it attained intensity with a minimum central pressure of 920 hPa and a maximum surface wind speed of 60 m/s. Saomai was the strongest typhoon that ever occurred over China's offshore region and the most powerful typhoon ever to have made landfall over mainland China. Zhejiang and Fujian were devastated by the storm and the State Flood Control and Drought Relief Headquarters said economic losses in the two provinces reached 11.3 billion yuan (US $1.4 billion). It added that 54,000 houses were destroyed, with 122,700 hectares (303,000 acres) of farmland ruined by the strong winds and floods. Saomai affected around 6 million people and displaced 1.7 million residents. At least 441 people were killed by the storm in China.

3 MODEL DESCRIPTION AND EXPERIMENTAL DESIGN

For numerical experiments, we use the ARW modeling system version 3.1 (Skamarock et al.[10]). We perform three-dimensional experiments by using two-way interactive nesting in two domains with horizontal grid spacing of 4.5 km (D1), and 1.5 km (D2), respectively. Figure 1a shows the location of domains, and the center of D1 is at 24.1°N and 127.8°E. The number of horizontal grid points is 500×300 and 421×421, for D1 and D2, respectively. The outer domain D1 is integrated from 1200 UTC 7 August to 1200 UTC 10 August 2006, and the inner domain starts at 0000 UTC 8 August. D2 is an automatic vortex-following moving nest grid so that the center of the domain is always located at the center of the typhoon. The model tracks the vortex center every 20 minutes and then the inner domain moves, if necessary. The vortex center is determined by finding the minimum geopotential height at 500 hPa. The advantage of using a moving frame is that the typhoon does not leave the domain during long-period experiments with a limited domain size. Forty-seven σ levels are used from the surface to the top at 50 hPa.

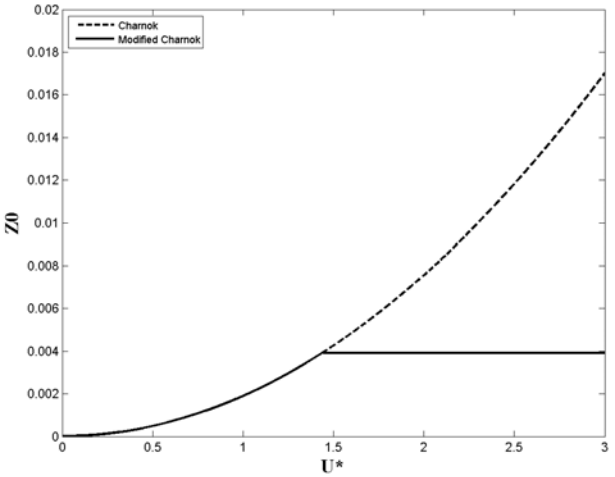

Figure 1. The surface roughness as a function of friction velocity. The dashed line denotes the Charnok formula and solid line denoted the modified Charnok formula.

The initial and boundary conditions for the ARW model experiments are derived from the Japan Meteorological Agency (JMA) Regional Spectral Model's (RSM) reanalysis field at 20 km×20 km resolution (JMA[11]; Hosomi[12]). The model physics options are the same for the two domains. The Rapid Radiative Transfer Model (RRTM) longwave radiation (Mlawer et al.[13]) and Dudhia shortwave radiation schemes (Dudhia[14]) are adopted. For the parameterization of turbulence in the PBL, the Yonsei University (YSU) scheme (Noh et al.[15]; Hong et al.[16]) is used. The mircophysics scheme is Purdue Lin scheme (Lin et al.[17]; Chen and Sun[18]), which includes six categories of hydrometeors: vapor, cloud water, rain, cloud ice, snow, and graupel.

To account for the effects of increasing roughness on the turbulent boundary layer over the ocean, ARW use a wind speed–dependent formula for the surface roughness (z_0), named Charnok[19] formula:

$$z_0 = c_{z_0}(u_*^2 / g) + o_{z_0}, \quad (1)$$

where c_{z_0}=0.0185 and $o_{z_0} = 1.59\times10^{-5}$; u_* is the friction velocity, g is the gravitational acceleration. The formulation cause z_0 to continue to increase with wind speed with no limit. Furthermore, the drag coefficient in the neutral condition can be defined as:

$$C_D = \left(\frac{k}{\ln \frac{10.0}{z_0}} \right)^2, \quad (2)$$

where k is the von Kármán constant. The 10-m drag coefficient can generally increase with the wind speed. However, Donelan et al.[8] has shown that C_D does not continue to increase with the wind speed greater than 30 m/s and levels off in laboratory experiments. Also the observation in State 973 Program suggests C_D remains near 0.0026 with high wind speeds (973 Evaluating Report) in the western North Pacific, and the observational research (Black et al.[20]) suggests the value near 0.003 in the Atlantic.

Based on the observation in State 973 Program, the Charnok formula is modified (Figure 1) by limiting z_0 to within the range of values of $0 \le z_0 \le 3.92\times10^{-3}$. This modified formula is applied to the YSU PBL scheme, which is referred hereafter to YSU modified experiment. And the control run uses the Charnok formula and the YSU PBL scheme, which is referred to YSU experiment.

4 MODEL VERIFICATION AND STRUCTURE OF BOUNDARY LAYER

4.1 *Track and intensity*

Figure 2 compares the simulated tracks from both experiments with the China Meteorological Administration/Shanghai Typhoon Institute (CMA-STI) best analysis from 0000 UTC 8 August to 1200 UTC 10 August. Typhoon Saomai (2006) kept moving northwestward during its lifecycle. The track forecasts in both experiments are quite similar, although the tracks are shifting a slightly northward than the best track. Both experiments reproduce the observed west-northwestward storm movement, which means that the steering flow produced by the background circulation is similar in both experiments.

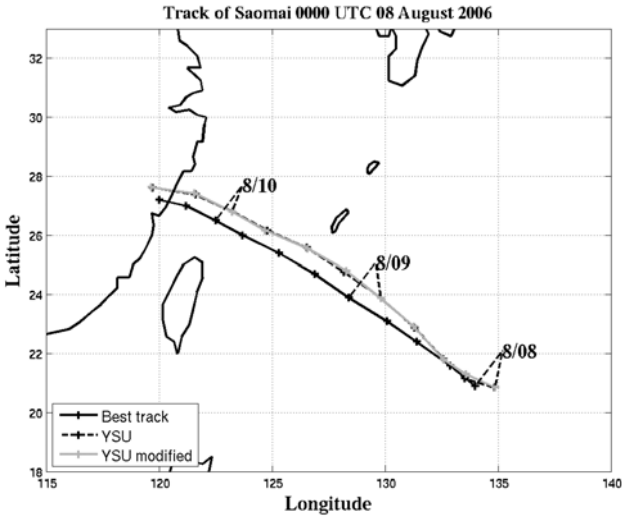

Figure 2. The tracks of Typhoon Saomai from the best track analysis (every 6 h) by JMA (2006) and the model experiments (every 6 h) from 0000 UTC 8 August to 1200 UTC 10 August 2006.

Figure 3 compares the time series of the simulated minimum sea level pressure and maximum surface wind from both experiments to the corresponding best analysis by CMA-STI. Because the model is initialized with JMA RSM reanalysis fields at 20 km×20 km resolution, there are no differences at the beginning of both experiments. Although all

experiments start from the same initial conditions, the intensity forecasts are different when wind speed is greater than 30 m/s, due to the modified formula at high wind speed. Overall, small differences in intensity of simulated typhoons are found in the first day, the typhoon of the YSU modified experiment continues to intensify and the minimum sea level pressure is close to the observation, but the typhoon of the YSU experiment dose not continue to intensify and is weaker than the observation. Afterward, the typhoon of the YSU modified experiment is the same as the observation when it moves into the coastal region, and both of them are weakened after landfall. The maximum surface wind speeds display similar characteristics, but the typhoon of the YSU experiment has weaker maximum surface wind speed compared to the observation.

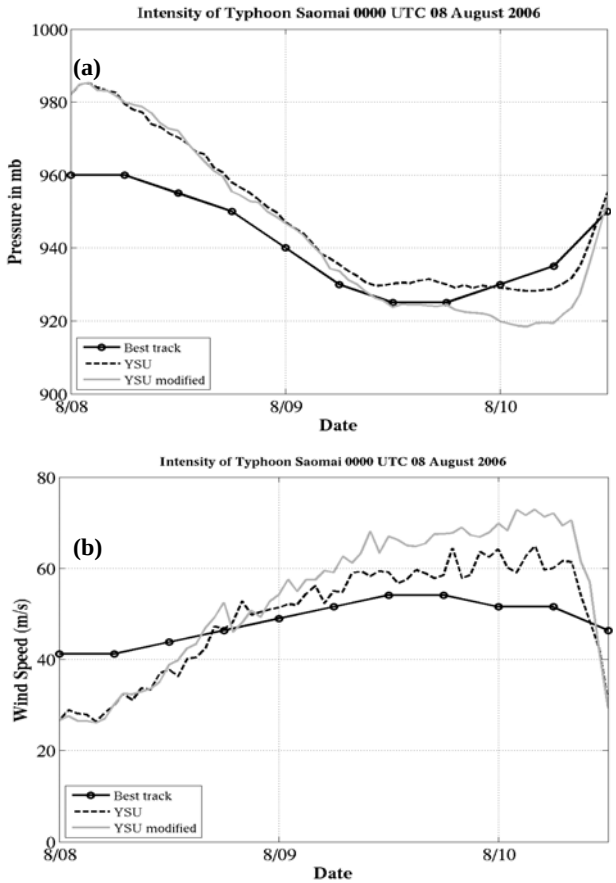

Figure 3. Time series of simulated (a) mimimum central pressure (hPa) and (b) maximum surface wind speed (m/s) of Saomai from 0000 UTC 08 August to 1200 UTC 10 August 2006 for both experiments and the corresponding best analysis by JMA.

4.2 *Radar reflectivity and surface wind speed*

Now let us shift our attention to the verification of the system scale features, such as the radar reflectivity and wind speed. The observed radar reflectivity (Zhao et al.[21]) and the simulated radar reflectivity image captured at 2 km valid at 1900 UTC 9 August are compared in Figure 4. Both experiments have larger eyes compared to the observation. The typhoon of the YSU modified experiment has closed and broader eyewalls with embedded cores of high reflectivity, and a spiral rainband is located in the east to south region relative to the eyewall, similar to the observation. The typhoon of the YSU experiment has looser and narrower eyewall. The high echo region is not closed and the magnitude of radar reflectivity is smaller. On the other hand, Figure 5 depicts the observed and simulated wind image captured at 1 km valid at 0349 UTC and 0400 UTC 10 August. Compared to the observation, magnitude of wind speed and strong wind area (>33 m/s) from two experiments are about twice the observation, but the location of maximum wind is the same as the observation, in the northeast part of inner core. In the YSU modified experiment, wind streaks exist in the south part of the eyewall, and the magnitudes of the streaks are 10–15 m/s larger relative to the surrounding areas, and the widths are about several ten kilometers and the azimuthal lengths are about a few hundred kilometers. They always exist in the lower layer of the eyewall across the whole life of the typhoon. The characteristics of our results are coincident with the experiment of Andrew using 2-km spacing (Yau et al.[22]). These small but intense wind streaks bring serious wind disasters and have been reported by observations and damage analysis mentioned in Yau et al.[22]. Comparing with the hourly rainfall (figure not shown), we find that the wind streaks correspond to the heavy rainfall areas. They cooperate with each other, causing various nature disasters.

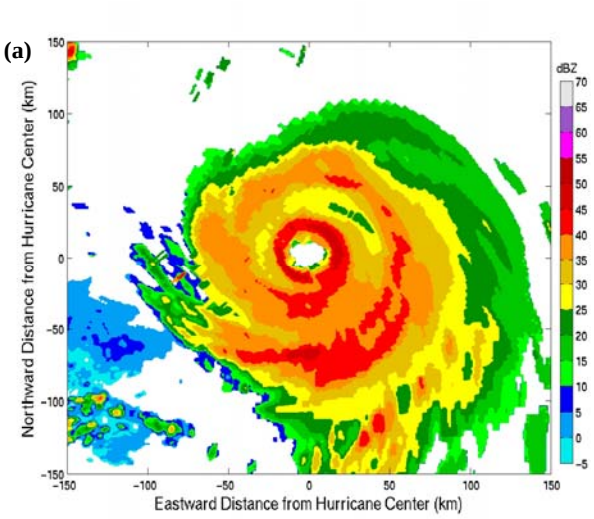

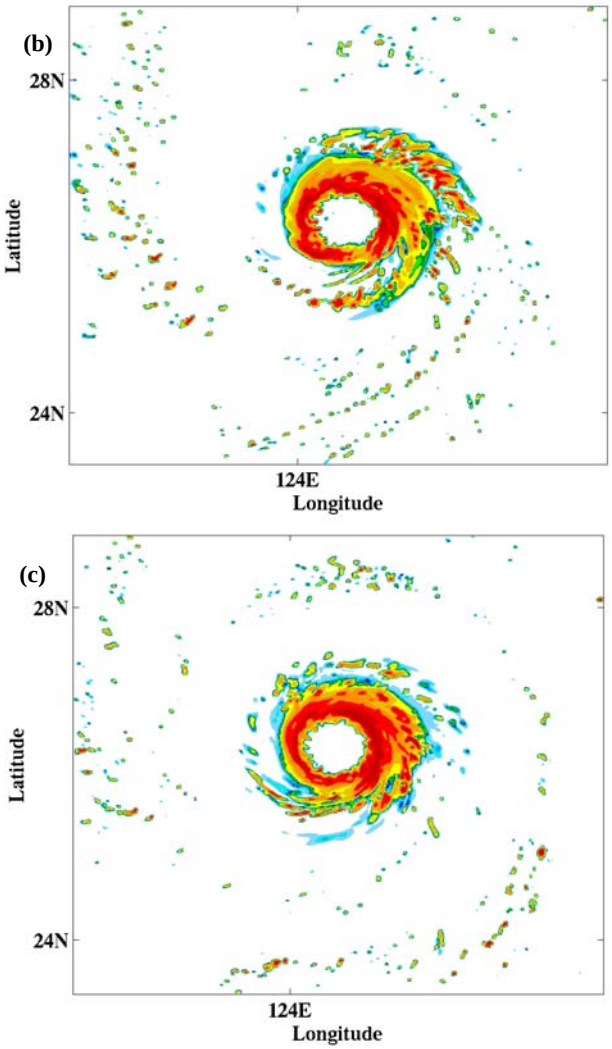

Figure 4. (a) 2-km height observed radar reflectivity (dBZ) at 1851 UTC 9 August, and 2-km height simulated radar reflectivity (dBZ) at 1900 UTC 9 August 2006 from (b) YSU, (c) YSU modified.

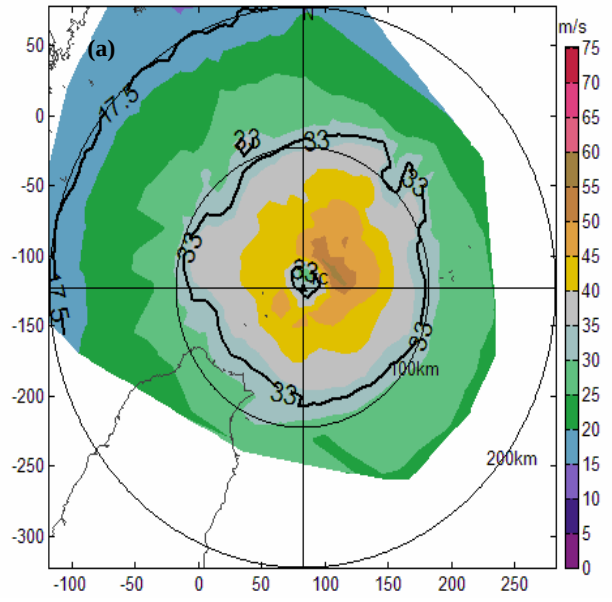

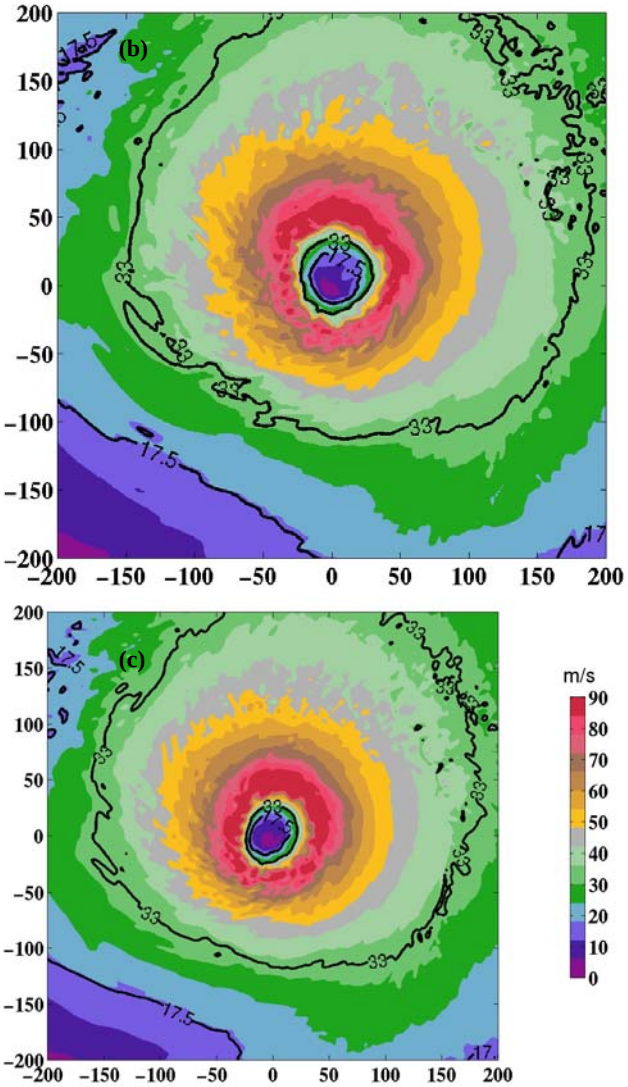

Figure 5. (a) 1-km height observed wind speed (m/s) at 0349 UTC 10 August, and 1-km height simulated wind speed (m/s) at 0400 UTC 10 August 2006 from (b) YSU, (c) YSU modified. 17.5 m/s and 33 m/s wind speed contour lines are highlighted.

4.3 C_D, C_K and surface flux

The relationship between C_D, C_K and wind speed valid at 1200 UTC 9 August 2006 is shown in Figure 6. In the YSU experiment, the Charnok formula is used and the surface roughness and C_D are increased with 10-m wind speed. The C_K is also increased slowly with wind speed, because the formula of C_K is

$$C_K = \left(\frac{k}{\ln\frac{10.0}{z_0}}\right)\left(\frac{k}{\ln\frac{10.0}{z_{0q}}}\right), \tag{3}$$

$$\ln\frac{10.0}{z_{0q}} = \ln\left(\frac{u_* \cdot k \cdot 10.0}{xka} + \frac{10.0}{z_0}\right), \tag{4}$$

where z_0 is the roughness length, z_{0q} is the thermal roughness length, u_* is the friction velocity, k is the von Kármán constant and xka is a constant that equals

to 2.4×10^{-5}. The thermal roughness length is more slowly varying than the roughness length, leading to slower increases of C_K with wind speed than that of C_D. In the YSU modified experiment, the Charnok formula is changed and the roughness is leveled off when wind speed is greater than 30 m/s, with C_D and C_K leveled off too. Compared to the YSU experiment, C_D is decreased more than C_K when wind speed is greater than 30 m/s.

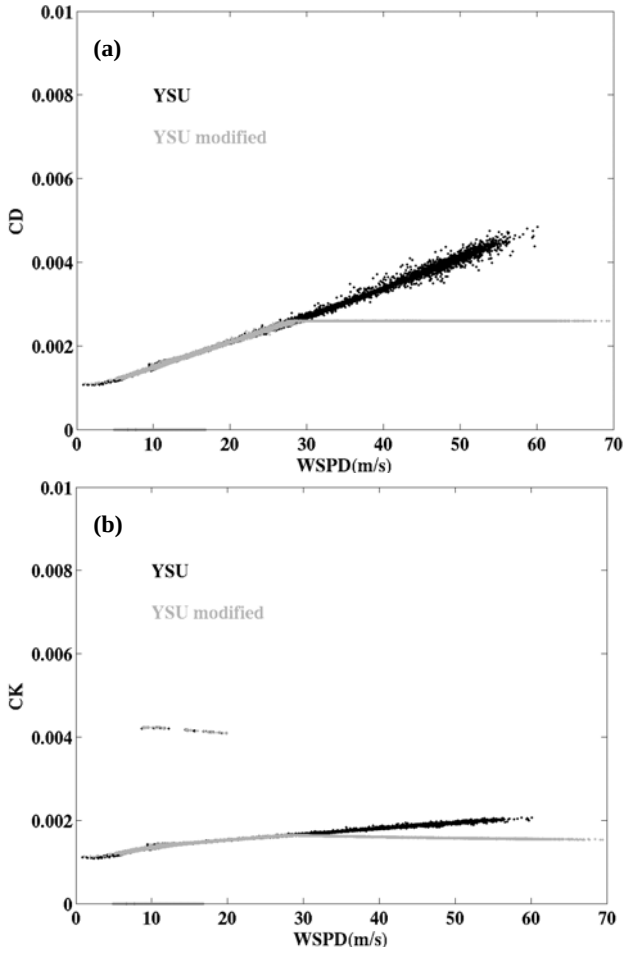

Figure 6. The simulated (a) drag coefficient and (b) enthalpy exchange coefficient as a function of 10-m wind speed from both experiments at 1200 UTC 9 August 2006.

The comparisons of horizontal distributions of 10-m wind speed and 0.25-km radar reflectivity valid at 1200 UTC 9 August 2006 are shown in Figure 7. Wind speeds in the YSU modified experiment are significantly higher than those in the YSU. The YSU modified experiment produces the asymmetry, and the maximum surface wind speed is located in the northeast part relative to the eye. The radius of maximum wind (RMW) is smaller than that in the YSU experiment. The peak winds in the YSU modified experiment are also higher, consistent with the smaller RMW, than those of the YSU experiment. Both experiments produce the echo-free eye, the closed eyewall with several high reflectivity bands, and intense convective regions around them. In the YSU modified experiment, high reflectivity regions exist in the northeast part of the eyewall, several spiral mesoscale high reflectivity bands are outside them, and there is a low reflectivity area between them. There is an echo-free region in the southwestern quarter and a series of spiral rainbands outside the eyewall.

Horizontal distributions of C_D and C_K valid at 1200 UTC 9 August 2006 are compared in Figure 8. Following the formula of C_D and C_K, the YSU modified produces smaller C_D and C_K than the YSU, especially in the high wind speed region. C_D is decreased more than C_K in the inner core region, and this change causes different surface fluxes and inner core structures. Figure 9 depicts the sensible heat flux and latent heat flux at the same time. The sensible heat flux in the YSU modified experiment is more in the northwestern part of the inner core, and the latent heat flux is smaller and its large value region is narrower than the counterparts in the YSU experiment. The magnitude of sensible heat flux is smaller than that of latent heat flux, and the total enthalpy flux of the YSU modified is smaller than the YSU, corresponding to reduced value of C_K. The wind speed is higher in the YSU modified experiment but the enthalpy flux is smaller, because C_D decreases more than C_K, so the typhoon in the YSU modified experiment is stronger than that in the YSU. The modified roughness length is able to produce stronger storm than the original one.

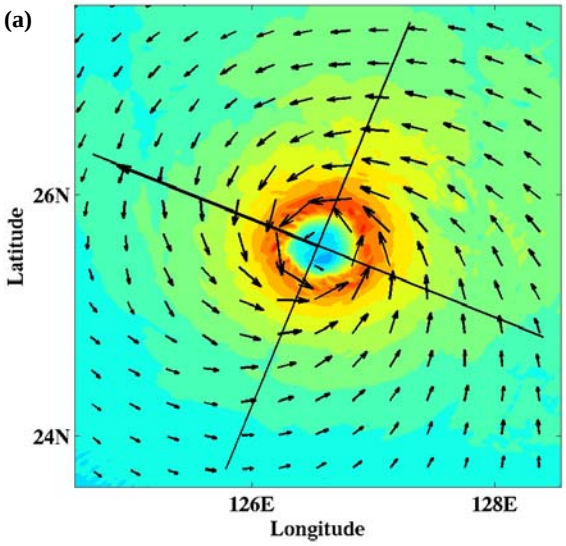

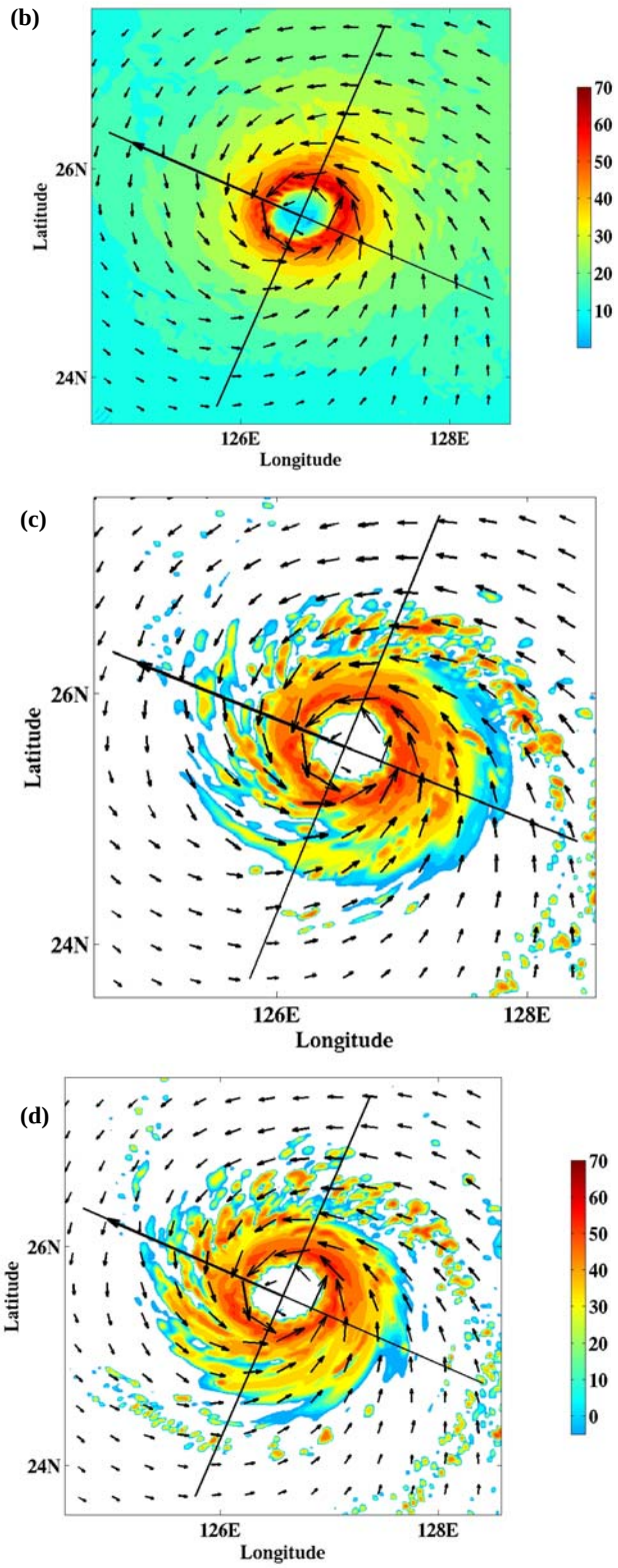

Figure 7. (a) The model simulated 10-m wind speed (shaded; m/s) and wind vectors (shafted arrows; m/s) at 1200 UTC 9 August 2006 from YSU; (b) same as (a) but for and YSU modified; (c) The model simulated 0.25-km radar reflectivity (shaded; dBZ) and wind vectors (shafted arrows; m/s) at 1200 UTC 9 August 2006 from YSU; (d) same as (c) but for and YSU modified. The big vector stands for the motion of storm.

4.4 *Azimuthally averaged structures*

Focusing on the lower levels, Figure 10 shows the azimuthally averaged wind and temperature fields in the low-level eyewall region for the two experiments at 1800 UTC 09 August. All azimuthally averaged fields are computed from 1.5-km grids, with the storm center defined at the location of the minimum surface pressure. The gray shadings are the azimuthal winds and the heavy contours are the radial winds with dashed contours indicating negative values in Figure 10a and 10b. The equivalent potential temperatures with gray shading are in Figure 10c and 10d.

It is fair to say that two experiments have consistent differences. The YSU modified experiment produces a significantly smaller RMW. The low-level radial inflow and the radial outflow at the top of the boundary layer are significantly stronger and slightly deeper in the YSU modified experiment than those in the YSU. Comparing the YSU modified with YSU experiments, the former produces slightly stronger lower level outflow (8 m/s) and substantially higher maximum winds than the latter.

For equivalent potential temperature (θ_e), both experiments are qualitatively consistent with each other in the outer region. The experiments show that the maximum θ_e is both at the surface center, and the higher values of θ_e in the YSU modified experiment extend farther upward in the lower level. It means that stronger outflow in the lower level can draw air out of the eye to reduce the central pressure, and transport high θ_e air from the bottom of the eye upwards to partially support eyewall convection. Both experiments show a region of strong vertical gradient and weak radial gradient of θ_e in the low-level inflow regions. Especially, there is stronger vertical gradient in the eyewall region of the YSU modified experiment. It means more unstable stratification and stronger upward motions in this area. They induce stronger secondary circulation and more intense development of the storm.

It is useful to compare the tendencies of wind, temperature, and moisture generated by the PBL schemes. Azimuthal averages of these tendencies at the 0.5-km height at 1800 UTC 9 August are shown in Figure 11. The wind speed tendencies for the two schemes have similar magnitudes, the YSU modified experiment has a stronger wind speed tendency, just localized inside the RMW and the YSU experiment has a smaller maximum value, localized at a larger distance from the storm center (Figure 11a). Both experiments show cooling at this layer, likely due to the upward mixing of high-θ_e air from the top of the mixed layer. The YSU experiment shows similar cooling but the magnitude is relatively much weaker. The turbulent moisture tendency in the eyewall is actually positive for both experiments, indicating that

upward water vapor transport is compensated by the convergence of large radial inward water vapor flux. As discussed earlier, the YSU modified experiment tends to produce a stronger radial inflow, radial outflow, and tangential wind maxima as compared to the YSU experiment, suggesting that the YSU modified experiment causes larger wind speed and water vapor tendencies and transports more high-θ_e air to the eyewall. It induces stronger convection in the eyewall, thereby leading to a stronger secondary circulation.

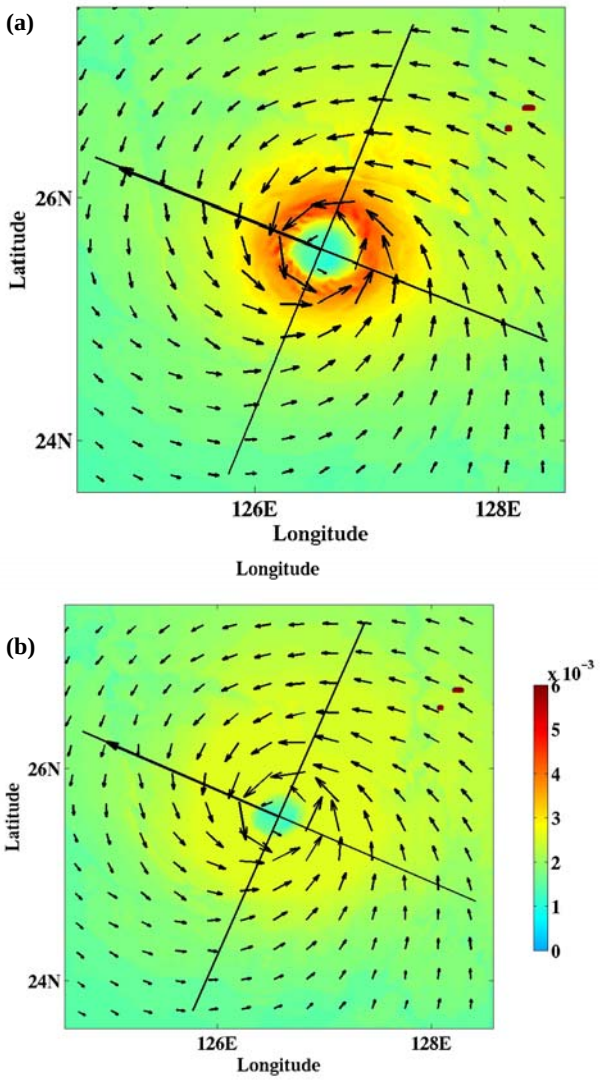

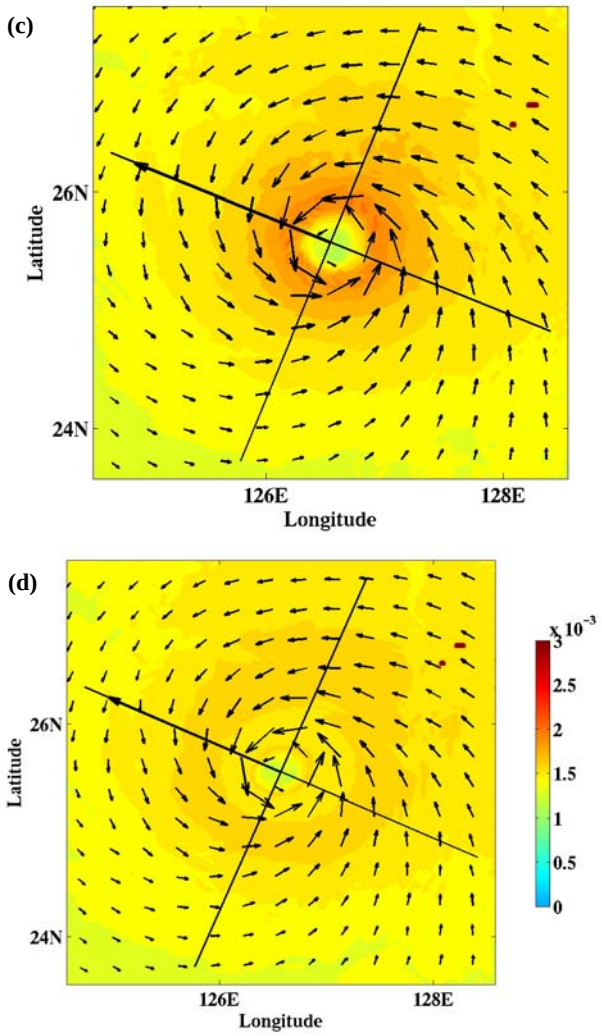

Figure 8. The model simulated drag coefficient (shaded) and wind vectors (shafted arrows; m/s) at 1200 UTC 9 August 2006 from YSU; (b) same as (a) but for the YSU modified; (c) The model simulated enthalpy exchange coefficient (shaded) and wind vectors (shafted arrows; m/s) at 1200 UTC 9 August 2006 from the YSU; (d) same as (c) but for the YSU modified. The big vector stands for the motion of storm.

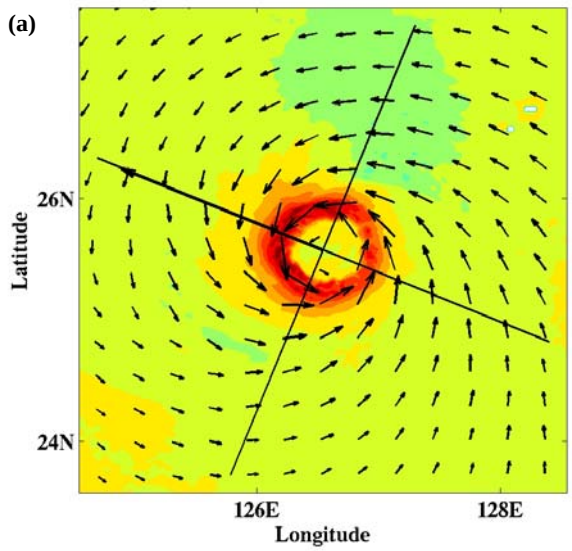

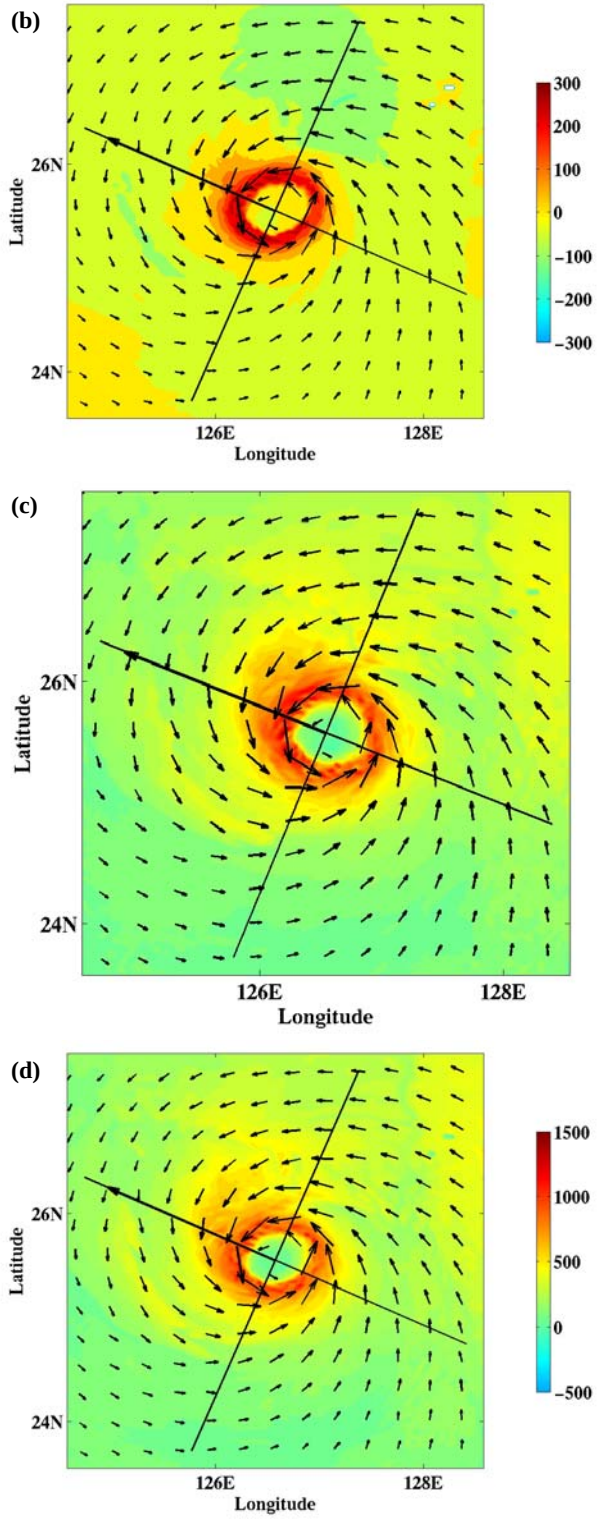

Figure 9. (a) The model simulated sensible heat flux (shaded; W/m^2) and wind vectors (shafted arrows; m/s) at 1200 UTC 9 August 2006 from YSU; (b) same as (a) but for the YSU modified; (c) The model simulated latent heat flux (shaded; W/m^2) and wind vectors (shafted arrows; m/s) at 1200 UTC 9 August 2006 from YSU; (d) same as (c) but for the YSU modified. The big vector stands for the motion of storm.

5 CONCLUDING REMARKS

In this study, two numerical experiments are conducted with the ARW model to simulate Typhoon Saomai (2006) and to examine the modified Charnok formula. Both experiments are integrated with the same initial conditions from the JMA RSM data fields, and use the moving nested version ARW model with the finest grid size of 1.5 km. The following points can be concluded:

(1) Modified Charnok formula cloud cause differences in the intensity of simulated typhoon, starting from 30-h into the integration, and has little sensitivity in tracks. The YSU modified experiment has a bigger deepening rate of simulated typhoon after 30- h and is the same as observation in the last 12 h. In contrast, the simulated typhoon in the YSU experiment dose not continue to intensify after 30-h and is weaker than the observation.

(2) Both experiments produce different structures of the boundary layer. The YSU modified experiment produces stronger storm, which has more compacted and broader eyewalls with embedded cores of high reflectivity. In the YSU modified experiment, wind streaks exist in the south part of the eyewall, and the magnitudes of the streaks are 10–15 m/s bigger relative to the surrounding areas, and the YSU experiment does not have this characteristics.

(3) In the YSU modified experiment, the roughness is leveled off when wind speed is greater than 30 m/s, and the C_D and C_K are leveled off too. Compared to the YSU experiment, C_D is decreased more than C_K when wind speed is greater than 30 m/s, and the YSU modified experiment produces more sensible heat flux and less latent heat flux.

(4) The YSU modified experiment has a significantly smaller RMW. The low-level radial inflow and the radial outflow at the top of the boundary layer in the YSU experiment are significantly stronger and slightly deeper relative to those in the YSU experiment. In the lower level, the YSU modified experiment has slightly stronger outflow and stronger vertical gradient of θ_e, as well as substantially higher maximum tangential winds than the YSU experiment has. The YSU modified experiment produces larger wind speed and water vapor tendencies and transports more high-θ_e air to the eyewall in the boundary layer. It also induces stronger convection in the eyewall, thereby leading to a stronger secondary circulation.

Based on the above results, we can deduce that the PBL scheme in the ARW system is not perfect. The modified relationship between wind speed and exchange coefficients are efficient for intensification of model typhoon during the summer monsoon season in the western North Pacific, compared to the original one. More observation of boundary layer in the eyewall are needed to perfect the PBL scheme, particularly the processes occurring in high wind speed, in order to improve the numerical prediction of

the typhoon intensity and structure. In addition, more investigation is certainly necessary for fully understanding the boundary layer structures and physical processes. In the forthcoming articles, we will focus on the structures of the boundary layer before and after the typhoon landfall.

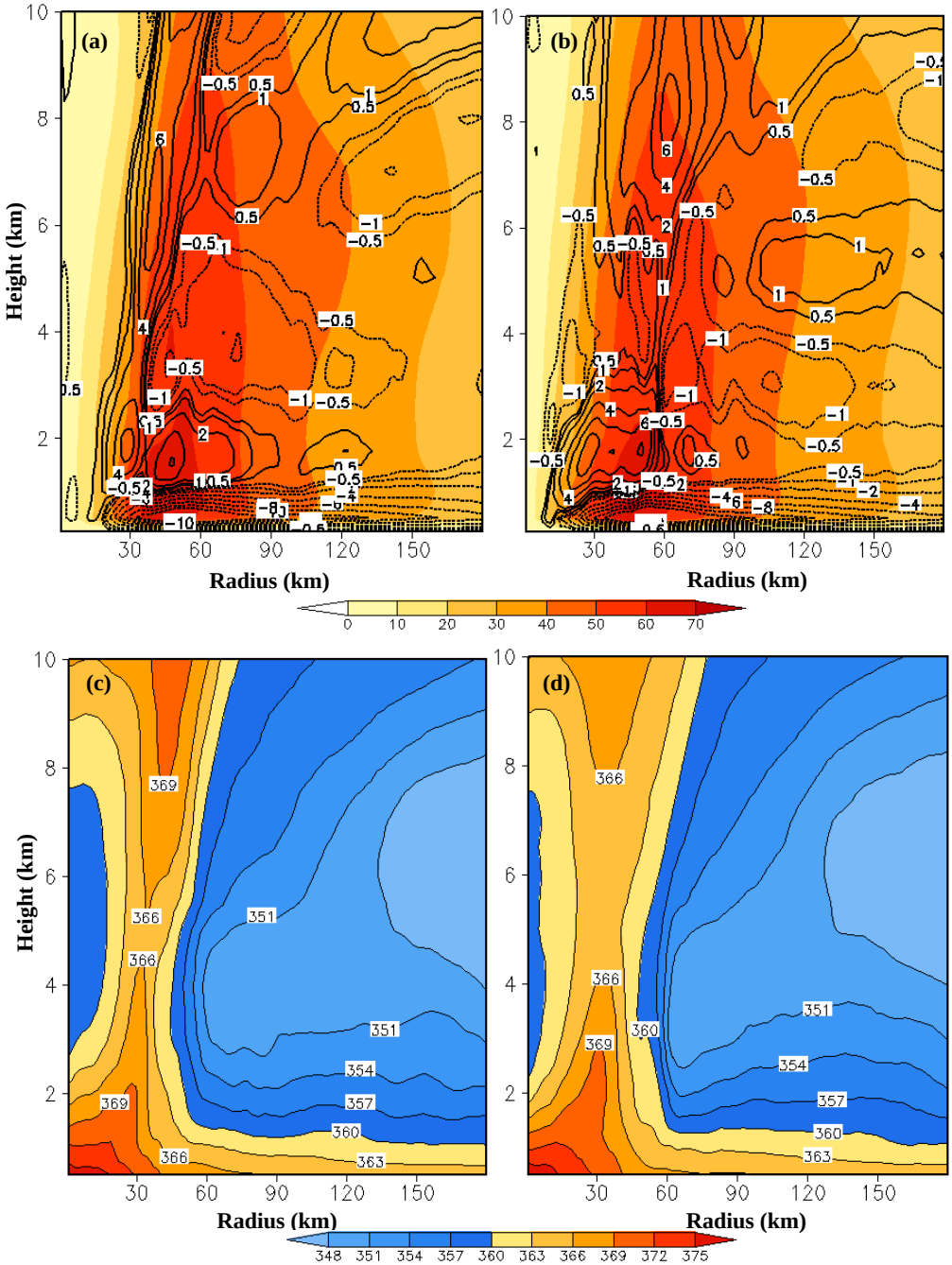

Figure 10. Azimuthally averaged azimuthal winds (shaded, m/s) and radial winds (contours, m/s) at 1800 UTC 9 August 2006 from (a) YSU and (b) YSU modified. Azimuthally averaged equivalent potential temperature (thin solid line with shades; K) at 1800 UTC 9 August 2006 from (c) YSU and (d) YSU modified.

REFERENCES:

[1] MALKUS J S, RIEHL H. On the dynamics and energy transformations in steady-state hurricanes [J]. Tellus, 1960, 12(1): 1-20.

[2] OOYAMA K V. Numerical experiment of the life cycle of tropical cyclones [J]. J. Atmos. Sci., 1969, 26(1): 3-40.

[3] EMANUEL K A. An air-sea interaction theory for tropical cyclones. Part I: Steady-state maintenance. [J]. J. Atmos. Sci., 1986, 43(6): 585-605.

[4] ROTUNNO R, EMANUEL K A. An air-sea interaction theory for tropical cyclones, Part II: Evolutionary study using axisymmetric nonhydrostatic numerical model. [J]. J. Atmos. Sci., 1987, 44(3): 542-561.

[5] ROSENTHAL S L. The response of a tropical cyclone model to variations in boundary layer parameters, initial conditions, lateral boundary conditions and domain size. [J]. Mon. Wea. Rev., 1971, 99(10): 767-777.

[6] EMANUEL K A. Sensitivity of tropical cyclones to surface exchange coefficients and a revised steady-state model

incorporating eye dynamics. [J]. J. Atmos. Sci., 1995, 52(22): 3969-3976.
[7] BRAUN S A, TAO W K. Sensitivity of high-resolution experiments of hurricane Bob (1991) to planetary boundary layer parameterizations. [J]. Mon. Wea. Rev., 2000, 128(12): 3941-3961.
[8] DONELAN M A, HAUS B K, REUL N, et al. On the limiting aerodynamic roughness of the ocean in very strong wind. [J]. Geophys. Res. Lett., 2004, 31, L18306, doi: 10.1029/2004GL019460.
[9] POWELL M D, VICKERY P J, REINHOLD T A. Reduced drag coefficient for high wind speeds in tropical cyclones. [J] Nature, 2003, 422: 279-283.
[10] SKAMAROCK W C, KLEMP J B, DUDHIA J, et al. A description of the advanced research WRF: Version 2 [R]. NCAR Tech. Note 468 1 STR, 2005, 88 pp.
[11] JMA. Outline of the operational numerical weather prediction at the Japan Meteorological Agency [J]. Appendix to WMO numerical weather prediction progress report, 2002.
[12] HOSOMI T. Implementation of targeted moisture diffusion for the JMA Regional Spectral Model (RSM). CAS/JSC WGNE [J]. Res. Act. Atmos. Ocean. Modeling, 2005, 35(5): 7-8.
[13] MLAWER E J, TAUBMAN S J, BROWN P D, et al. Radiative transfer for inhomogeneous atmospheres: RRTM, a validated correlated-k model for the longwave. [J]. J. Geophys. Res., 1997, 102 (D14), 16663-16682.
[14] DUDHIA J. Numerical study of convection observed during the winter monsoon experiment using a mesoscale two dimensional model. [J]. J. Atmos. Sci., 1989, 46(20): 3077-3107.
[15] NOH Y, CHEON W G, HONG S Y, et al. Improvement of the K-profile model for the planetary boundary layer based on large eddy experiment data. [J]. Bound.-Layer Meteor., 2003, 107(2): 421–427.
[16] HONG S Y, NOH Y, DUDHIA J. A new vertical diffusion package with an explicit treatment of entrainment processes [J]. Mon. Wea. Rev., 2006, 134(9): 2318-2341.
[17] LIN Y L, FARLEY R D, ORVILLE H D. Bulk parameterization of the snow field in a cloud model [J]. J. Climate Appl. Meteor., 1983, 22(6): 1065-1092.
[18] CHEN S H, SUN W Y. A one-dimensional time dependent cloud model. [J]. J. Meteor. Soc. Japan, 2002, 80(1): 99-118.
[19] CHARNOK H. Wind stress on a water surface [J]. Quart. J. Roy. Meteor. Soc., 1955, 81(350): 639-640.
[20] BLACK P G, D'ASARO E, DRENNAN W M, et al. Air-sea exchange in hurricanes: Synthesis of observations from the Coupled Boundary Layer Air-Sea Transfer experiment [J]. Bull. Amer. Meteor. Soc., 2007, 88(350): 357-374.
[21] ZHAO K, LEE W C, JOU J D. Single Doppler radar observation of the concentric eyewall in Typhoon Saomai [J]. 2006, near landfall, [J]. Geophys. Res. Lett., 2008, 35, L07807, doi:10.1029/2007GL032773.
[22] YAU M K, LIU Y, ZHANG D L, et al. A multiscale study of Hurricane Andrew (1992). Part VI: Small-scale inner-core structures and wind streaks [J]. Mon. Wea. Rev., 2004, 132(6): 1410-1433.

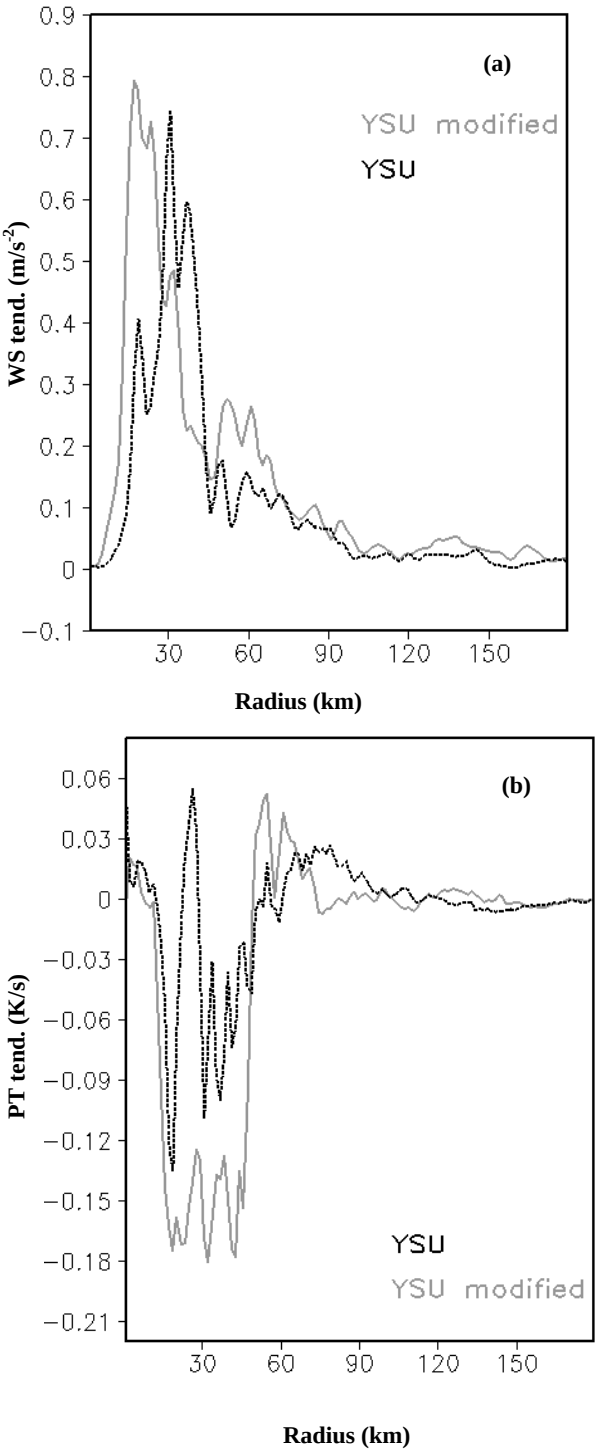

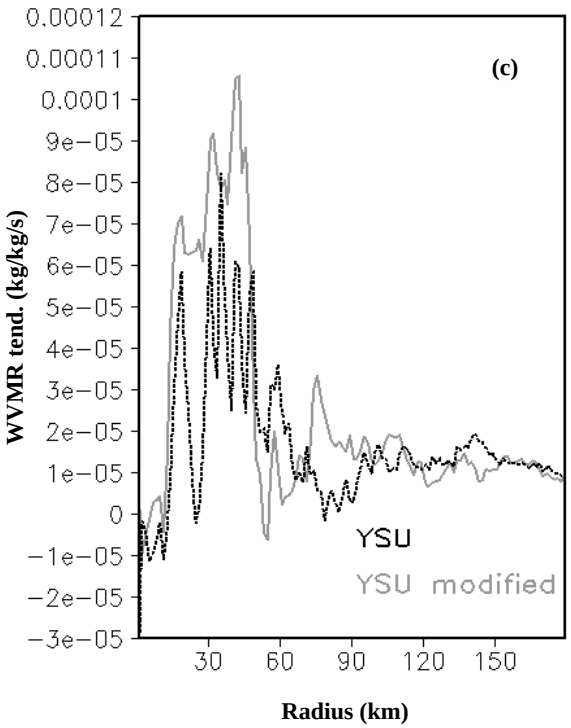

Figure 11. Azimuthally averaged tendencies of (a) wind speed (m/s^{-2}), (b) potential temperature (K/s) and (c) water vapor mixing ratio (kg/kg/s) at the 0.5-km height level at 1800 UTC 9 August 2006 from YSU and YSU modified experiments.

Citation: MING Jie, SONG Jin-jie, CHEN Bao-jun et al. Boundary layer structure in Typhoon Saomai (2006): Understanding the effects of exchange coefficient. *J. Trop. Meteor.*, 2012, 18(2): 195-206.